International Journal of the Physical Sciences Vol. 6(10), pp. 2541-2549, 18 May, 2011
Available online at http://www.academicjournals.org/IJPS
DOI: 10.5897/IJPS11.307
ISSN 1992 - 1950 ©2011 Academic Journals

Full Length Research Paper

A numerical study of steady state exothermic reaction in a slab with convective boundary conditions

A. M. K. Legodi and O. D. Makinde*

Institute for Advance Research in Mathematical Modelling and Computations, Cape Peninsula University of Technology, P. O. Box 1906, Bellville 7535, South Africa.

Accepted 4 April, 2011

In this paper, we considered a steady state, exothermic nth order oxidation chemical reaction in a slab with reactant consumption in the presence of convective heat and oxygen exchange with the surrounding ambient at the slab surface. The coupled nonlinear differential equations governing the system are obtained and are solved numerically using the standard Newton–Raphson shooting method along with a fourth-order Runge–Kutta integration algorithm. A perturbation method together with a special type of Hermite-Padé series summation and improvement technique is also employed to tackle the problem. Important properties of the temperature field including the effects of embedded parameters on the thermal stability of the system are discussed.

Key words: Rectangular slab, reactant consumption, thermal criticality, Hermite-Padé series, shooting method, convective boundary conditions.

INTRODUCTION

Studies related to thermal stability and heat transfer in a combustible material subjected to oxidation chemical reaction is aimed at ensuring the safety of its storage, transportation and usage. It is an important practical aspect of reactive hazard assessment (Lohrer et al., 2005; Tanaka et al., 2003; Bowes, 1984). Many studies have been conducted to determine the critical conditions that separate explosive and non-explosive domains of a proceeding reaction and evaluation of induction period of an explosion if it appears (Simmie, 2003; Balakrishnan et al., 1996; Makinde, 2004). Two main approaches are used for obtaining the necessary data. They are based either on direct determination of the explosion characteristics by means of explosive experiments (Warnatz et al., 2001). or on application of theoretical calculations (Bebernes and Eberly, 1989). One of the most important advantages of theoretical methods is that they can be applied as soon as a kinetic model had been evaluated from data from laboratory scale kinetic experiments. In particular, they allow estimation of runaway parameters in the earliest stages of the life cycle of a chemical product, thus ensuring elimination or significant reduction of the necessity for explosive experiments (Williams, 1985). Moreover, the approach based on the mathematical theory of combustion unites the two branches of theoretical approach, that is, the family of semi-analytical methods and more sophisticated numerical simulation methods. The grounds for the semi-analytical simplified theories developed by Semenov (1956). Frank-Kamenetskii (1969) and others are well known. They give convenient approximate analytical relations that do not require complicated calculations and are currently used as a rule for estimation of critical parameters. However, the application domain of these theories is essentially limited; therefore many practical problems cannot be solved due to high nonlinearity in their models without applying comprehensive techniques that require the use of numerical calculations. One such trend is related to a novel hybrid of numerical-analytical schemes known as Hermite-Padé approximation approach (Makinde and Osalusi, 2005; Makinde, 2006, 2007; Sergeyev and Goodson, 1998). This approach, over the last few years, has proved itself as a powerful benchmarking tool and a potential alternative to traditional numerical techniques in various applications in sciences and engineering.

*Corresponding author. E-mail: makinded@cput.ac.za.

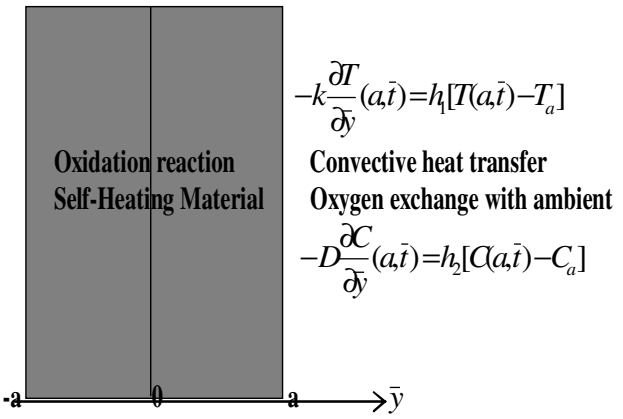

Figure 1. Geometry of the problem.

The objective of this study is to investigate the combined effects of convective heat and oxygen exchange with the ambient on the nth order exothermic oxidation chemical reaction and thermal stability in a slab of combustible material.

MATHEMATICAL MODEL

The geometry of the problem is depicted in Figure 1. It is assumed that the combustible material is undergoing an nth order oxidation chemical reaction. The complicated chemistry involved in the problem is simplified by assuming a one-step finite-rate irreversible reaction between the combustible material (hydrocarbon) and the oxygen of the air, that is:

$$C_iH_j+\left(i+\frac{j}{4}\right)O_2\rightarrow iCO_2+\frac{j}{2}H_2O+Heat$$

(Combustible material + oxygen → heat + carbon dioxide + water)

Following Simmie (2003), Balakrishnan et al. (1996), Makinde (2004), Bebernes and Eberly (1989), and Williams (1985) the steady state nonlinear differential equations describing the energy balance and oxygen concentration in the combustible material can be written as:

$$k\frac{d^2T}{d\bar{y}^2}+QA\left(\frac{KT}{\upsilon l}\right)^m(C-C_0)^n e^{-\frac{E}{RT}}=0, \quad (1)$$

$$D\frac{d^2C}{d\bar{y}^2}-A\left(\frac{KT}{\upsilon l}\right)^m(C-C_0)^n e^{-\frac{E}{RT}}=0, \quad (2)$$

with convective boundary conditions as Tshehla et al. (2010).

$$-k\frac{dT}{d\bar{y}}=h_1[T-T_a],\ -D\frac{dC}{d\bar{y}}=h_2[C-C_a],\ \text{at}\ \ \bar{y}=a \quad (3)$$

$$\frac{dT}{d\bar{y}}=\frac{dC}{d\bar{y}}=0,\qquad \bar{y}=0, \quad (4)$$

where T is the absolute temperature, T_a is the ambient temperature, C_a is the oxygen concentration in the surrounding air, C_0 is the initial concentration of oxygen in the material, T_0 is the slab initial temperature, k is the thermal conductivity of the material, Q is the exothermicity, A is the rate constant, E is the activation energy, R is the universal gas constant, l is the Planck's number, K is the Boltzmann's constant, v is the vibration frequency, a is the slab half width, $\bar{y}$ is the distance measured in the transverse direction, h_1 is the heat transfer between the material and its surroundings, D is the diffusivity of oxygen in the material, h_2 is the transfer of oxygen from the material to its surroundings, n is the chemical reaction order and m is the numerical exponent such that m ={-2, 0, ½} represent numerical exponent for Sensitized, Arrhenius and Bimolecular kinetics respectively (Balakrishnan et al., 1996; Makinde, 2004; Bebernes and Eberly, 1989). We introduce the following dimensionless variables into Equations 1 to 4.

$$Bi=\frac{h_1a}{k},\gamma=\frac{h_2a}{D},\phi=\frac{(C-C_0)}{(C_a-C_0)},\theta=\frac{E(T-T_0)}{RT_0^2},\theta_a=\frac{E(T_a-T_0)}{RT_0^2},y=\frac{\bar{y}}{a}, \quad (5)$$
$$\varepsilon=\frac{RT_0}{E},\alpha=\frac{k}{D\rho c_p},\lambda=\frac{QAEa^2(C_a-C_0)^n}{kRT_0^2}\left[\frac{KT_0}{\upsilon l}\right]^m e^{-\frac{E}{RT_0}},\beta=\frac{kRT_0^2}{DQE(C_a-C_0)},$$

and we obtain the dimensionless governing equations as:

$$\frac{d^2\theta}{dy^2}+\lambda(1+\varepsilon\theta)^m\phi^n e^{\frac{\theta}{(1+\varepsilon\theta)}}=0, \quad (6)$$

$$\frac{d^2\phi}{dy^2}-\lambda\beta(1+\varepsilon\theta)^m\phi^n e^{\frac{\theta}{(1+\varepsilon\theta)}}=0. \quad (7)$$

The associated boundary conditions (3) to (4) become:

$$\frac{d\theta}{dy}=-Bi[\theta-\theta_a],\ \frac{d\phi}{dy}=-\gamma[\phi-1]\qquad \text{at}\quad y=1, \quad (8)$$

$$\frac{d\theta}{dy}=\frac{d\phi}{dy}=0,\qquad \text{at}\quad y=0, \quad (9)$$

where λ, ε, β, γ, Bi represent the Frank-Kamenetskii parameter, activation energy parameter, Oxygen consumption rate parameter, mass Biot number and the thermal Biot number respectively. A body of material releasing heat to its surroundings may achieve a safe steady-state where the temperature of the body reaches some moderate value and stabilizes. However, when the rate of heat generation of the material exceeds the rate of heat loss to the surroundings, then ignition can occur. In the study, Equations 6 to 9 are solved using perturbation method.

PERTURBATION METHOD

Due to the nonlinear nature of the temperature and reacting species concentration Equations in (6) and (7), it is convenient to seek a solution in the form a power series expansion in parameter λ, that is:

$$\theta=\sum_{i=0}^{\infty}\theta_i\lambda^i, \qquad \phi=\sum_{i=0}^{\infty}\phi_i\lambda^i \tag{10}$$

Substituting the solution series in Equation (10) into Equations (6) to (9) and collecting the coefficients of like powers of λ, we obtained the followings:

Order zero (that is, coefficient of λ to power zero from the series)

$$\frac{d^2\theta_0}{dy^2}=0, \quad \frac{d^2\phi_0}{dy^2}=0 \tag{11}$$

with $\frac{d\theta_0}{dy}(1)=-Bi[\theta_0(1)-\theta_a]$, $\frac{d\phi_0}{dy}(1)=-\gamma[\phi_0(1)-1]$

, $\frac{d\theta_0}{dy}(0)=\frac{d\phi_0}{dy}(0)=0$. (12)

Order one (that is, coefficient of λ to power one from the series)

$$\frac{d^2\theta_1}{dy^2}=-(1+\varepsilon\theta_0)^m\phi_0^n e^{\frac{\theta_0}{(1+\varepsilon\theta_0)}}, \tag{13}$$

$$\frac{d^2\phi_1}{dy^2}=\beta(1+\varepsilon\theta_0)^m\phi_0^n e^{\frac{\theta_0}{(1+\varepsilon\theta_0)}}=0, \tag{14}$$

with $\frac{d\phi_1}{dy}(1)=-\gamma\phi_1(1)$, $\frac{d\theta_1}{dy}(1)=-Bi\theta_1(1)$,

$\frac{d\theta_1}{dy}(0)=\frac{d\phi_1}{dy}(0)=0$. (15)

Order two (that is, coefficient of λ to power two from the series)

$$\frac{d^2\theta_2}{dy^2}=-(1+\varepsilon\theta_0)^m\phi_0^n e^{\frac{\theta_0}{(1+\varepsilon\theta_0)}}\left[\frac{\theta_1}{(1+\varepsilon\theta_0)^2}+n\frac{\phi_1}{\phi_0}+\frac{m\varepsilon\theta_1}{(1+\varepsilon\theta_0)}\right], \tag{16}$$

$$\frac{d^2\phi_2}{dy^2}=\beta(1+\varepsilon\theta_0)^m\phi_0^n e^{\frac{\theta_0}{(1+\varepsilon\theta_0)}}\left[\frac{\theta_1}{(1+\varepsilon\theta_0)^2}+n\frac{\phi_1}{\phi_0}+\frac{m\varepsilon\theta_1}{(1+\varepsilon\theta_0)}\right], \tag{17}$$

with $\frac{d\phi_2}{dy}(1)=-\gamma\phi_2(1)$, $\frac{d\theta_2}{dy}(1)=-Bi\,\theta_2(1)$,

$\frac{d\theta_2}{dy}(0)=\frac{d\phi_2}{dy}(0)=0$. (18)

and so on. The above equations for the coefficients of solution series are solved iteratively for the temperature fields and reacting species concentration, we obtain:

$$\theta(y)=\theta_a-\frac{\lambda}{2\,Bi}\left(1+\varepsilon\theta_a\right)^m e^{\frac{\theta_a}{1+\varepsilon\theta_a}}\left(y^2\,Bi-2-Bi\right)+O\left(\lambda^2\right) \tag{19}$$

$$\phi(y)=1+\frac{\lambda\beta}{2\gamma}\left(1+\varepsilon\theta_a\right)^m e^{\frac{\theta_a}{1+\varepsilon\theta_a}}\left(y^2\gamma-2-\gamma\right)+O\left(\lambda^2\right) \tag{20}$$

Using a computer symbolic algebra package (MAPLE), the first few terms of the above solution series in Equations (19) to (20) are obtained. We are aware that these power series solutions are valid for very small parameter values of λ. However, using Hermite-Padé series summation and improvement technique, we have extended the usability of the solution series beyond small parameter values as illustrated in the following section.

HERMITE-PADÉ APPROXIMATION TECHNIQUE

From the application point of view, it is very important to determine the appearance of criticality or non-existence of steady-state solution for certain parameter values. In order to achieve this, we first derived a special type of Hermite-Padé approximant (Makinde, 2004, 2007; Sergeyev and Goodson, 1998). Let:

$$U_N(\lambda)=\sum_{n=0}^{N}a_n\lambda^n+O(\lambda^{N+1}), \qquad \text{as } \lambda\to 0, \tag{21}$$

be a given partial sum. It is important to note here that Equation (21) can be used to approximate any output of the solution of the problem under investigation (example, the series for the wall heat flux parameter in terms of Nusselt number Nu = - dθ/dy at y = 1), since everything can be Taylor expanded in the given small parameter. Assume U (λ) is a local representation of an algebraic function of λ in the context of nonlinear problems, we seek an expression of the form:

$$F_d(\lambda,U)=\sum_{m=1}^{d}\sum_{k=0}^{m}f_{m-k,k}\lambda^{m-k}U^k, \tag{22}$$

of degree d ≥ 2, such that:

$$\frac{\partial F_d}{\partial U}(0,0)=1 \quad \text{and } F_d(\lambda,U_N)=O(\lambda^{N+1}), \text{ as } \lambda\to 0. \tag{23}$$

The requirement (23) reduces the problem to a system of N linear equations for the unknown coefficients of F_d. The entries of the underlying matrix depend only on the N given coefficients a_n and we shall take $N=(d^2+3d-2)/2$, so that the number of equations equals the number of unknowns. The polynomial F_d is a special type of Hermite-Padé approximant and is then

Table 1. Comparison between analytical and numerical results ($\lambda=\beta=\gamma=0.1$, $\varepsilon=0$, $n=2$, $Bi=\theta_a=1$).

y	θ(y) Perturbation results	θ(y) Numerical results	$\left\|\theta_{numer.}-\theta_{perturb.}\right\|$
0	1.32892926	1.32892929	3.0×10^{-8}
0.1	1.32780785	1.32780788	3.0×10^{-8}
0.2	1.32444550	1.32444553	3.0×10^{-8}
0.3	1.31884776	1.31884779	3.0×10^{-8}
0.4	1.31102389	1.31102392	3.0×10^{-8}
0.5	1.30098675	1.30098677	2.0×10^{-8}
0.6	1.28875273	1.28875276	3.0×10^{-8}
0.7	1.27434168	1.27434170	2.0×10^{-8}
0.8	1.25777674	1.25777676	2.0×10^{-8}
0.9	1.23908423	1.23908425	2.0×10^{-8}
1.0	1.21829349	1.21829351	2.0×10^{-8}

Table 2. Computations showing the criticality procedure rapid convergence ($\beta=0.1$, $\gamma=Bi=\theta_a=n=1$, $\varepsilon=0$).

d	N	θ_{max}	λ_{cN}
2	4	2.133563429	0.111399437253
3	8	2.245843906	0.111399418112
4	13	2.245636361	0.111399421506
5	19	2.245636371	0.111399421512
6	26	2.245636371	0.111399421512

investigated for bifurcation and criticality conditions using Newton diagram, Vainberg and Trenogin [16].

NUMERICAL APPROACH

The numerical technique chosen for the solution of the coupled ordinary differential Equations (6) and (7) is the standard Newton–Raphson shooting method along with a fourth-order Runge–Kutta integration algorithm. Equations (6) to (7) are transformed into a system of first order differential equations as follows:

Let $\theta=x_1$, $\theta'=x_2$, $\phi=x_3, \phi'=x_4$, where the prime symbol represent derivatives with respect to *y*. Then, the problem becomes:

$$x_1'=x_2, \qquad x_2'=-\lambda(1+\varepsilon x_1)^m x_3^n e^{\frac{x_1}{(1+\varepsilon x_1)}}, \qquad x_3'=x_4,$$

$$x_4'=\lambda\beta(1+\varepsilon x_1)^m x_3^n e^{\frac{x_1}{(1+\varepsilon x_1)}}, \tag{24}$$

subject to the following initial conditions:

$$x_1(0)=s_1, x_2(0)=0, x_3(0)=s_2, x_4(0)=0. \tag{25}$$

The unspecified initial conditions s_1 and s_2 are guessed systematically and Equation (24) is then integrated numerically as initial valued problems until the given boundary conditions at y =1 are satisfied. For each set of parameter values for λ, ε, β, γ and Bi, the procedure is repeated until conditions at the y = 1 are satisfied and the desired degree of accuracy (namely 10^{-7}) of the results obtained is achieved.

RESULTS AND DISCUSSION

In this study, we validate the above theoretical results using physically realistic values of various embedded parameters in the numerical experiment. It is important to note that increasing parameter value of λ indicates an increase in the rate of exothermic chemical kinetics in the slab. A comparison between the results obtained using the partial sum involving the first 20 terms of the perturbation series solution and purely fourth-order Runge–Kutta numerical integration coupled with shooting method at small and moderate values of embedded parameters are shown in Table 1. Generally, the difference is of order 10^{-8} and a perfect agreement is noticed.

In order to obtain the thermal stability criterion in the reacting slab, the Hermite-Padé approximation procedure in Hermite-Padé approximation technique was applied to the first few terms of the solution series in perturbation method.and we obtained the results as shown in Tables 2 and 3.

The results in Table 2 reveal the rapid convergence of

Table 3. Computations showing thermal ignition criticality for different parameter values.

Bi	γ	β	n	θ_a	m	ε	θ_{max}	λ_c
0.1	1	0.01	1	1.0	0.0	0.00	2.0172018519	0.01310984287
1	1	0.01	1	1.0	0.0	0.00	2.1163034602	0.10058516043
10	1	0.01	1	1.0	0.0	0.00	2.2127440013	0.27532575932
100	1	0.01	1	1.0	0.0	0.00	2.2200715856	0.32658480960
∞	1	0.01	1	1.0	0.0	0.00	2.2205606260	0.33330414740
1	5	0.01	1	1.0	0.0	0.00	2.1098592062	0.09999778812
1	10	0.01	1	1.0	0.0	0.00	2.1090640021	0.09992508139
1	1	0.05	1	1.0	0.0	0.00	2.1666489097	0.10496770865
1	1	0.10	1	1.0	0.0	0.00	2.2456363719	0.11139942151
1	1	0.01	3	1.0	0.0	0.00	2.1395726916	0.10267041887
1	1	0.01	5	1.0	0.0	0.00	2.1638439062	0.10484446876
1	1	0.01	1	0.5	0.0	0.00	1.6163034602	0.16583689354
1	1	0.01	1	0.1	0.0	0.00	1.2163034602	0.24739957357
1	1	0.01	1	1.0	0.0	0.01	2.1633708697	0.10474696724
1	1	0.01	1	1.0	0.5	0.01	2.1572733201	0.10368955515
1	1	0.01	1	1.0	-2.0	0.01	2.1884248614	0.10911552331
1	1	0.01	1	1.0	0.0	0.10	2.7942887760	0.15217860387

Hermite-Padé approximation procedure with gradual increase in the number of series coefficients utilized in the approximants. In Table (3), it is noteworthy that the magnitude of thermal ignition criticality (λ_c) increases with an increase in the thermal Biot number (Bi >0) due to convective cooling and a decrease in the oxygen supply from the surrounding ambient represented by a decrease in parameter value of γ. This invariably will lead to a delay in the development of thermal runaway in the reacting slab and enhances thermal stability. Similar effect of thermal stability enhancement is observed with increasing parameter values of β, n, ε and a decrease in the value of ambient temperature parameter θ_a. Thus, higher order oxidation chemicals kinetic augment thermal stability. It is worth mentioning that a combined increase in the parameter values of γ, θ_a together with a decrease in the parameter values of Bi, β, n, and ε can cause a decrease in the magnitude of thermal criticality parameter (λ), leading to early development of thermal ignition in the system. Furthermore, it is interesting to note from Table (3) that thermal ignition occur faster in a bimolecular (m=0.5) type of exothermic oxidation reaction as compared to the Arrhenius (m=0) and sensitized (m=-2) type of reaction. A slice of the bifurcation diagram for $0 \leq \varepsilon << 1$ in the (λ, θ_{max}) plane is shown in Figure (2). It represents the qualitative change in the thermal system as the parameter (λ) increases.

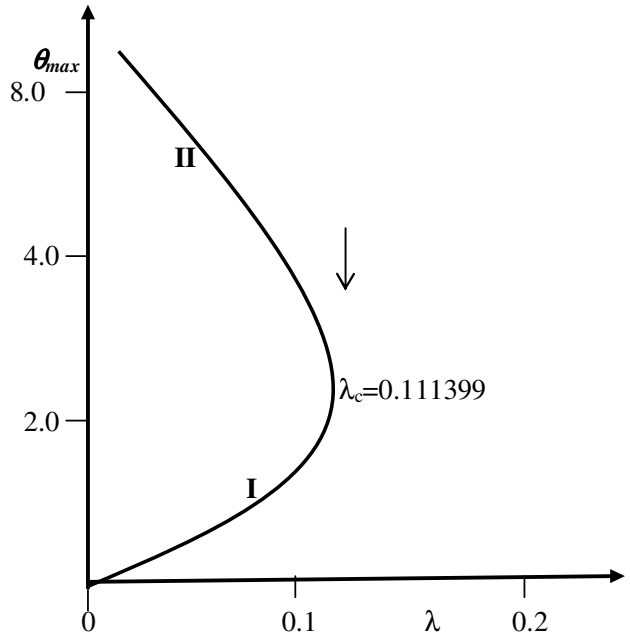

Figure 2. A slice of approximate bifurcation diagram in the (λ, θ_{max}) plane when $\beta = 0.1$, $\varepsilon = 0$, $\gamma = Bi = \theta_a = n = 1$.

In particular, for $0 \leq \varepsilon << 1$, Bi > 0, β > 0, γ > 0 and n > 0, there is a critical value λ_c (a turning point) such that, for $0 < \lambda < \lambda_c$ there are two solutions (labeled I

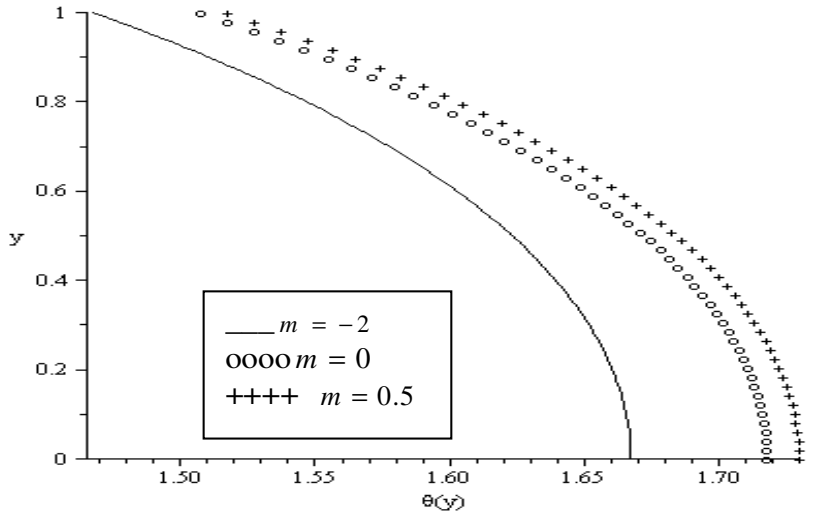

Figure 3. Temperature profiles for n =2, $\beta=\lambda=\gamma=Bi=\theta_a=1$, $\varepsilon=0.1$.

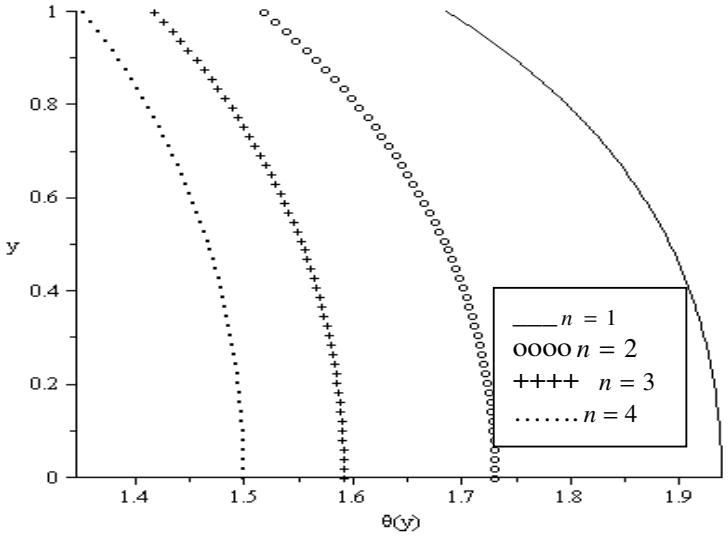

Figure 4. Temperature profiles for m=0.5, $\beta=\lambda=\gamma=Bi=\theta_a=1$, $\varepsilon=0.1$.

and II). The upper and lower solution branches occur due to the nonlinearity in the temperature dependent chemical kinetics in the governing equations for energy and concentration balance. When $\lambda > \lambda_C$ the system has no real solution and displays a classical form indicating thermal runaway. As exothermic reaction due to oxidation chemical kinetics increases, the slab temperature increases uncontrollably until it ignites.

Effect of various parameters on temperature profiles

Figures (3) to (8) illustrate the effects of various thermophysical parameters on the steady state slab temperature profiles. The temperature is maximum along the slab centerline and minimum at the slab surface due to convective heat transfer to the ambient. Figure (3) shows that the slab temperature is highest during bimolecular reaction (m = 0.5) and lowest for sensitized reaction (m=-2), hence confirming the earlier results in the literature (Makinde, 2004). This observation is also in agreement with the results highlighted in Table (3). In Figures (4) to (6), we observe that the slab temperature decreases with an increase in the values of reaction order index (n), Biot number (Bi) and the oxygen consumption rate parameter (β). This confirms the results in Table (3)

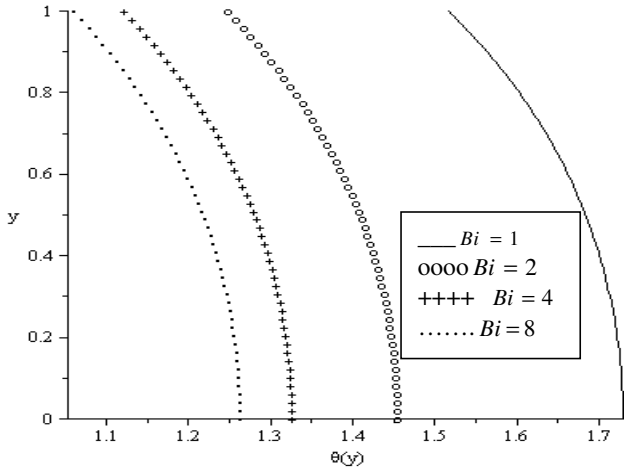

Figure 5. Temperature profiles for n=2, m=0.5, $\beta=\lambda=\gamma=\theta_a=1$, $\varepsilon=0.1$.

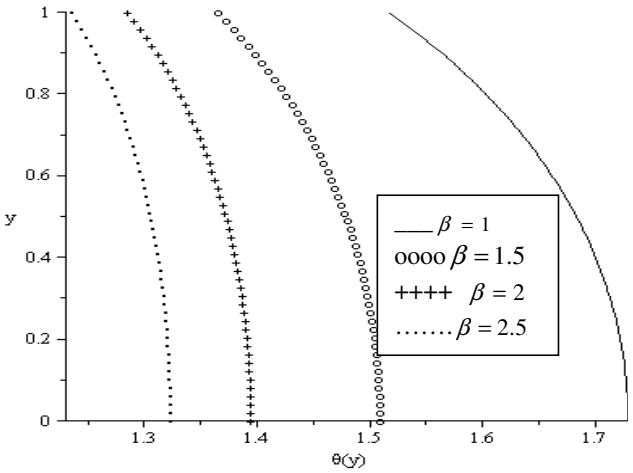

Figure 6. Temperature profiles for n = 2, m=0.5, $\lambda=Bi=\gamma=\theta_a=1$, $\varepsilon=0.1$.

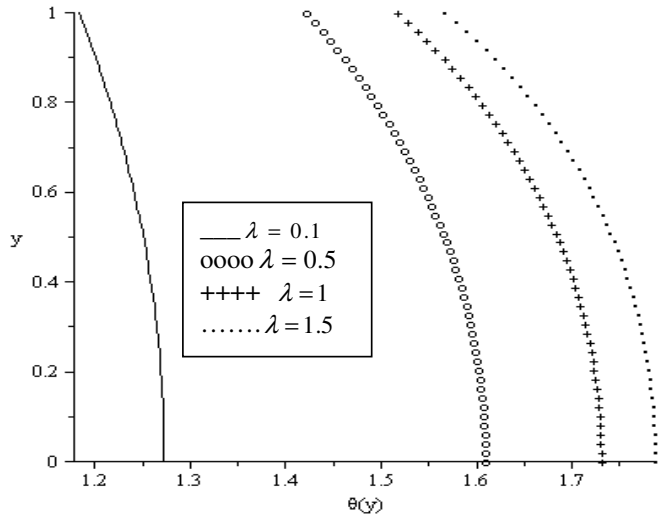

Figure 7. Temperature profiles for n = 2, m = 0.5, $\beta = Bi = \gamma = \theta_a = 1$, $\varepsilon = 0.1$.

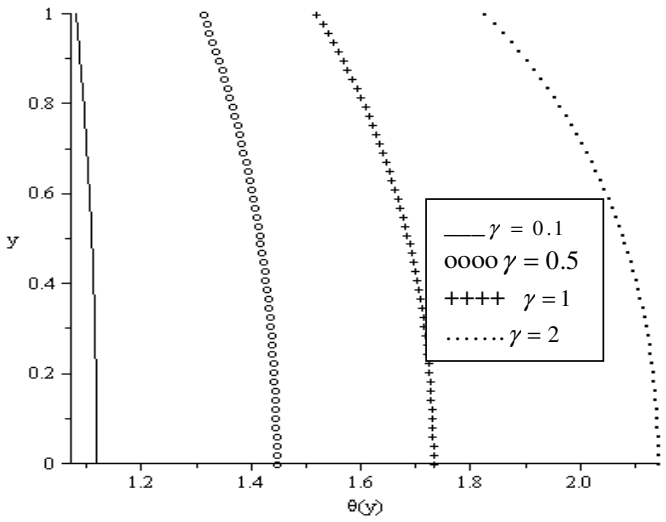

Figure 8. Temperature profiles for n = 2, m=0.5, $\beta=Bi=\lambda=\theta_a=1$, $\varepsilon=0.1$.

that a higher order exothermic oxidation chemical reaction will be more thermally stable than a lower one. The decrease in the slab temperature with increasing Biot number can be attributed to the action of convective cooling at the slab surface. As β increases the oxygen concentration in the interior of the slab decreases leading to a decrease in the slab temperature. Figures (7) to (8) show that the slab temperature increases with an increase in the parameter values of λ and γ. As the Frank-Kamenetskii parameter (λ) increases, the slab internal heat generation due to exothermic oxidation reaction increases, this invariably leads to an elevation in the slab temperature. An increase in the parameter value of γ implies an increase in the supply of oxygen from the ambient to support the reaction process (since oxygen is needed and very essential for this exothermic chemical reaction), leading to more internal heat been generated in the system and high temperature of the slab.

Effect of various parameters on Oxygen concentration profiles

Figures (9) to (14) illustrate the oxygen concentration profiles within the slab for different values of physical parameters. The concentration of oxygen is lowest along

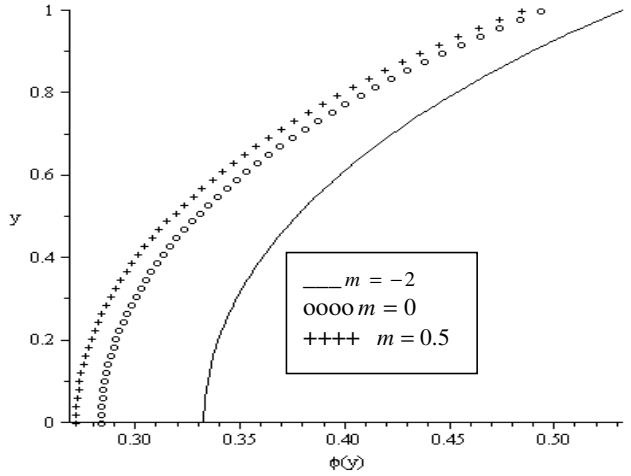

Figure 9. Oxygen concentration profiles for n=2, $\beta=\lambda=\gamma=Bi=\theta_a=1$, $\varepsilon=0.1$.

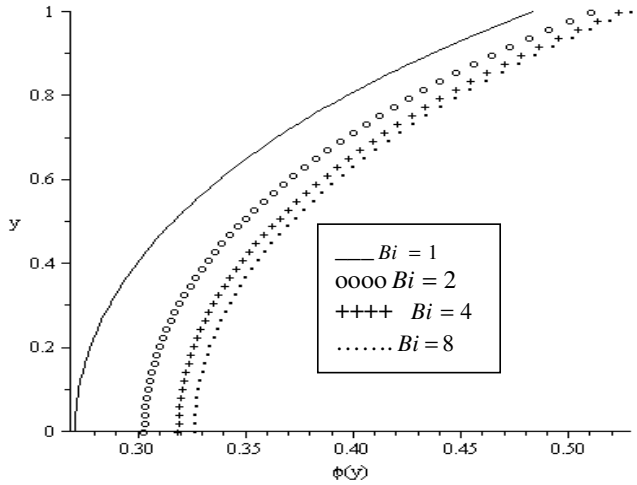

Figure 11. Oxygen concentration profiles for n = 2, m=0.5, $\beta=\lambda=\gamma=\theta_a=1$, $\varepsilon=0.1$.

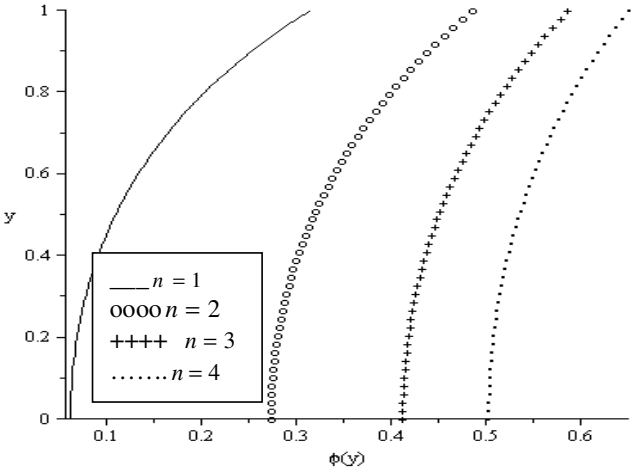

Figure 10. Oxygen concentration profiles for m=0.5, $\beta=\lambda=\gamma=Bi=\theta_a=1$, $\varepsilon=0.1$.

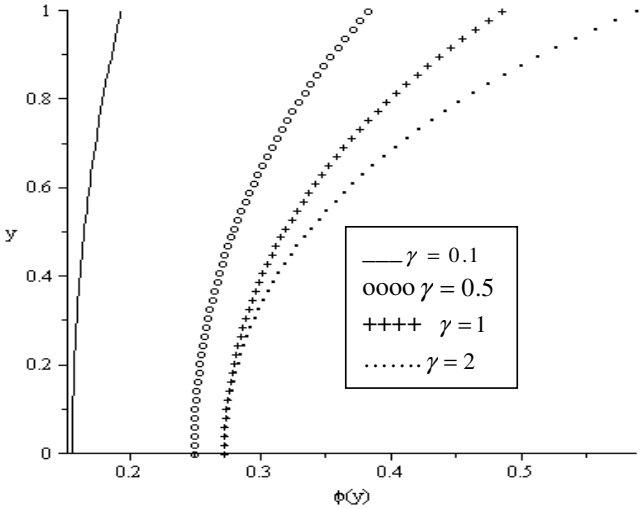

Figure 12. Oxygen concentration profiles for n = 2, m=0.5, $\beta=Bi=\lambda=\theta_a=1$,$\varepsilon$ =0.1.

slab centerline and highest at the slab surface due to exchange of oxygen at the slab surface with its surrounding ambient. Figure (9) shows that the oxygen concentration in the slab is lowest during bimolecular reaction (m = 0.5) and highest for sensitized reaction (m = -2). This can be attributed to the fact that oxygen consumption within the slab is highest during bimolecular chemical reaction leading to large internal heat generation and high depletion in oxygen concentration. In Figures (10) to (12), we observe that the oxygen concentration in the slab increases with an increase in the values of reaction order index (n), Biot number (Bi) and the slab surface oxygen supply rate parameter (γ). This implies that less oxygen is consumed in the system during a higher order exothermic oxidation chemical reaction, leading to a high level of oxygen concentration in the system than that of a lower reaction order. The increase in the oxygen concentration with increasing values Biot number and slab surface oxygen transfer parameter can be attributed to the combined effect of convective cooling and continuous supply of oxygen from the ambient at the slab surface. Figures (13) to (14) show that the oxygen concentration in the slab decreases with an increase in the parameter values of λ and β. As Frank-Kamenetskii parameter (λ) increases, more oxygen is consumed to support high rate of chemical reaction, this invariably leads to a depletion in the slab oxygen concentration. Similarly, as parameter value of β increases,

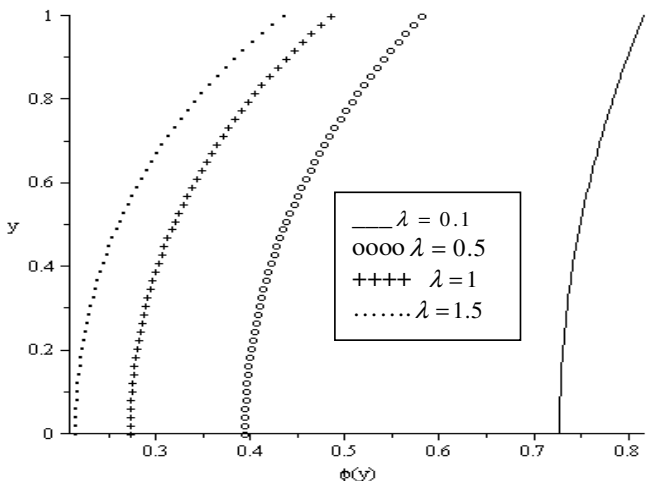

Figure 13. Oxygen concentration profiles for n = 2, m=0.5, β=Bi=γ=θ_a=1, ε =0.1.

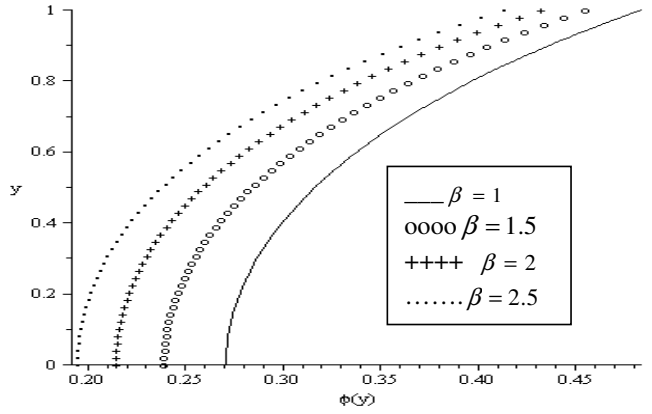

Figure 14. Oxygen concentration profiles for n = 2, m=0.5, λ=Bi=γ=θ_a=1, ε=0.1.

oxygen consumption increases, leading to a decrease in the slab oxygen concentration.

Conclusion

Analysis has been carried out for steady state nth order exothermic chemical reaction in a slab of combustible material, taking the diffusion and consumption of the reactant into account. The nonlinear differential equations governing the problem are solved numerically using Newton–Raphson shooting method along with a fourth-order Runge–Kutta integration algorithm. A bifurcation study by analytic continuation of a perturbation series in the bifurcation parameter for a particular solution branch is performed using a special type of Hermite-Padé series summation and improvement technique. The procedure reveals accurately the steady state thermal criticality conditions as well as the solution branches. The effects of various embedded parameters on the system are displayed graphically. Our results reveal among others, that the slab temperature is highest while the oxygen concentration is lowest during bimolecular reaction in comparison to Arrhenius and sensitized types of chemical reaction.

ACKNOWLEDGEMENT

The authors would like to thank the National Research Foundation (NRF) of South Africa Thuthuka programme for their generous financial support.

REFERENCES

Balakrishnan E, Swift A, Wake GC (1996). Critical values for some non-class A geometries in thermal ignition theory. Math. Comput. Modell., 24: 1–10.

Bebernes J, Eberly D (1989). Mathematical problems from combustion theory. Springer-Verlag, New York.

Bowes PC (1984). Self-heating: Evaluating and controlling the hazard. Amsterdam: Elsevier Sciences.

Frank Kamenetskii DA (1969). Diffusion and heat transfer in chemical kinetics. Plenum Press, New York.

Lohrer C, Schmidt M, Krause U (2005). A study on the influence of liquid water and water vapour on the self-ignition of lignite coal – experiments and numerical simulations. J. Loss Prevent Proc. Ind., 18(3): 167–177.

Makinde OD (2004). Exothermic explosions in a slab: A case study of series summation technique. Int. Comm. Heat Mass Trans., 31(8): 1227-1231.

Makinde OD (2006). Thermal ignition in a reactive viscous flow through a channel filled with a porous medium. Trans. ASME – J. Heat Trans., 128: 601-604.

Makinde OD (2007). Solving microwave heating model in a slab using Hermite-Pade approximation technique. Appl. Therm. Eng., 27: 599-603.

Makinde OD, Osalusi E (2005). Exothermic explosions in symmetric geometries-an exploitation of perturbation technique. Rom. J. Phys., 50(5-6): 581-584.

Semenov NN (1956). Some problems in chemical kinetics and reactivity. Princeton University press, Princeton, USA.

Sergeyev AV, Goodson DZ (1998). Summation of asymptotic expansions of multiple valued functions using algebraic approximations-application to a harmonic oscillator. J. Phys., A31: 4301-4317.

Simmie JM (2003). Detailed chemical kinetic models for the combustion of hydrocarbon fuels. Prog. Energy Combust. Sci., 29: 599–634.

Tanaka S, Ayala F, Keck JC (2003). A reduced chemical kinetic model for HCCI combustion of primary reference fuels in a rapid compression machine. Combust. Flame, 133: 467–481.

Tshehla MS, Makinde OD, Okecha GE (2010). Heat transfer and entropy generation in a pipe flow with temperature dependent viscosity and convective cooling. Sci. Res. Essays, 5(23): 3730-3741.

Vainberg MM, Trenogin VA (1974). Theory of branching of solutions of nonlinear equations. Noordoff, Leyden.

Warnatz J, Maas U, Dibble R (2001). Combustion: Physical and chemical fundamentals, modeling and simulation, experiments, pollutant formation, Springer-Verlag Berlin and Hiedelberg GmbH and Co. K.

Williams FA (1985). Combustion theory. Second Edition, Benjamin & Cuminy publishing Inc. Menlo Park, Califonia.